Analysis of Agglomerate Size from Burning Aluminized AP/RDX/HTPB Propellants in Quench Bomb

Tai-Kang Liu* and Chi-Fa Hsieh†
Chung Shan Institute of Science and Technology, Lungtan, Taiwan 32526, Republic of China

Introduction

KNOWLEDGE of the aluminum oxide particle size emerging from the propellant burning surface is important for predicting combustion stability, combustion efficiency, insulator erosion, and the performance of a solid rocket motor loaded with highly aluminized propellant. Different types of laboratory apparatus have been employed to collect the solid combustion products for subsequent determination of particle size and unburned aluminum fraction. Among these apparatus, some[1,2] use only stationary parts, whereas some[3-6] use a rotating bowl that can generate centrifugal forces to the quench fluid inside the bowl so that a thin layer of the liquid climbs the vertical bowl wall surface opposite the burning surface of the propellant sample. The quench fluid has the function of being able to stop the aluminum combustion reaction and neutralize the acidity of the combustion products.

Results of the effect of quench distance on the mean agglomerate size obtained from quench particle collection bomb (QPCB) experiments have rarely been reported. Churchill et al.[3] took account of the aluminum finite burning rate in QPCB by deriving the momentum conservation equation for the burning particle. Change in aluminum particle diameter as a function of distance from propellant surface was predicted. However, their assumption of continuous change of agglomerate size during oxidation is worth examining experimentally. Salita[5] obtained the variation of mass mean agglomerate size with a quench distance of 1, 3, and 6 in. for ammonium perchlorate (AP) composite propellant under pressures from 50 to 1000 psi. Independence of agglomerate size on quench distance was demonstrated for a quench distance greater than 1 in. The burning surface agglomerate size was calculated from the solid performance prediction (SPP) program.

The objective of this study is to analyze the agglomerate size from burning aluminized AP/cyclotrimethylene trinitramine (RDX)/hydroxy-terminated polybutadiene (HTPB) propellants in a QPCB. Our previous QPCB measurements[6] of agglomerate size have been reported at four pressures for a propellant formulation containing a variety of RDX and fine AP sizes as well as AP coarse/fine ratios and two aluminum powders, but only at a single quench distance (40 mm). This Note extends those results to as many as eight quench distances (7–77 mm) for three aluminum powders and two pressures. Figure 1 shows the QPCB sketch. The QPCB has a 2.5-l free volume. Furthermore, a comparison between the measured agglomerate sizes with the ones from theoretical predictions will be presented.

Received Nov. 14, 1994; revision received Feb. 16, 1996; accepted for publication Feb. 16, 1996.

*Senior Scientist, Chemical System Research Division. Member AIAA.
†Research Technician, Chemical System Research Division.

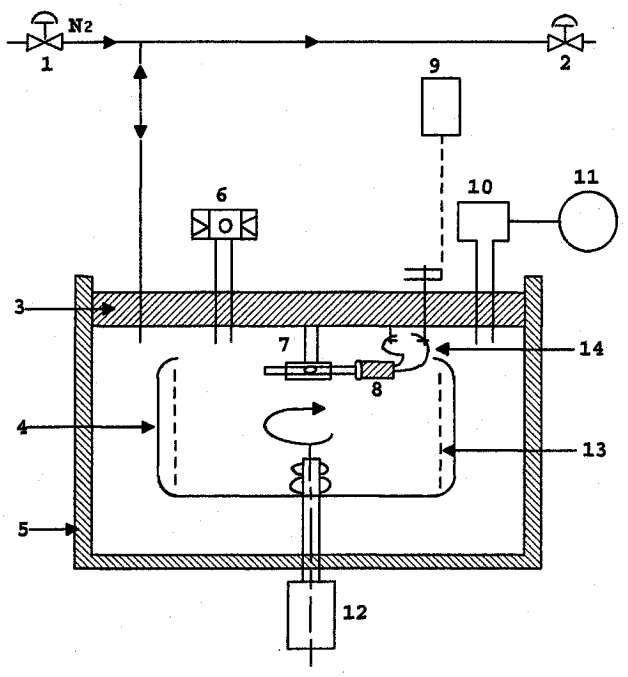

Fig. 1 QPCB schematic illustration: 1, pressurization valve; 2, exhaust valve; 3, cover plate; 4, rotation bowl; 5, QPCB body; 6, rupture disc; 7, adjustable sample holder; 8, propellant sample; 9, ignition dc power supply; 10, pressure sensor; 11, pressure indicator; 12, motor; 13, buffer solution layer; and 14, tungsten wire.

Experimental

The propellants tested in this investigation contain AP (49.6%), RDX (21.4%), HTPB (12%), and Al (17%), with a theoretical I_{sp} of 266 s at 1000 psi. Parameters for systematic investigations include, aluminum size in the propellant formulation (7, 17, and 30 μm); QPCB operation pressure (300 and 1000 psi of N_2); and quench distance from the propellant initial surface to quench fluid (2, 12, and 22 mm for 17- and 30-μm Al, 2–72 mm for 7-μm Al). Since the cylindrical propellant samples (6.28 mmϕ) are 10 mm long, the average quench distances were approximated as 7, 17, and 27 mm for 17- and 30-μm Al size propellants, and 7, 17, . . . , 77 in eight distances for 7-μm Al size propellant. Some of these distances are closer to the quench liquid than previous investigations[4-6] so that a maximum extent of agglomerate size change may be expected within these distance ranges. The weight mean agglomerate size was determined by passing the collected residues through a stack of 10 sieves (45, 88, . . . , 1400 μm) under ultrasonic vibration, further weighting the residues retained on each sieve. The mean agglomerate size was calculated by

$$D_{\exp} = \frac{\sum (\text{weight of particle in given size range}) \times (\text{midrange diameter})}{\sum \text{weight of particle in given size range}} \tag{1}$$

After the size determination, the collected sample was used for unburned aluminum measurement by the titration method as in our previous study.[6] This enables one to calculate the fraction of aluminum agglomerate that burns and converts to smoke by

$$F_s = 1 - \frac{\text{collected residue weight} \times \text{unburned Al fraction}}{\text{sample weight} \times 0.17} \tag{2}$$

Details on the operation of QPCB can be found in a previous paper.[6]

Results and Discussion

Figure 2 shows the accumulative size distribution of agglomerates for some propellants at two different pressures. A log-normal distribution is indicated, in agreement with previous investigations[3-5] without nitramine in the propellants. Figure 2 demonstrates that the agglomerate size decreases with increasing pressure. This is logical because less time will be available for the aluminum particles to melt and agglomerate on the burning surface for the higher burning rate propellants under the higher operating pressure. Figure 2 also shows that larger aluminum particles produced smaller agglomerates at both pressures, especially at higher pressure. This is because the smaller degree of melting for larger aluminum particles on the burning surface compared with the smaller aluminum particles.

Figure 3 shows the variation of mean agglomerate size vs quench distance for propellants with 7-μm aluminum. Each data point was obtained by averaging the repeated experiments shown in Table 1. Because of the presence of RDX in the propellant formulation, a melt layer was evidenced on the burning surface from the authors' previous investigation.[6] The melt can cover a part of the AP flame, thus decreasing the propellant burning rate. Furthermore, aluminum particles, especially the small diameter ones, tend to melt and agglomerate in the melt phase from the high temperature and sticky characteristics of the melt. These scenarios contribute to the larger agglomerate size shown in Fig. 3 compared with the ones[3-5] without RDX in the propellant formulation. The agglomerate size in Fig. 3 is found to be independent of quench distance for a distance greater than about 17–27 mm, in agreement with Salita[5] who reported the independence of the agglomerate size vs distance for a distance longer than 1 in. Figure 3 also demonstrates the larger variation of the agglomerate size at distances closer to the burning surface, a result that has rarely been reported in QPCB experiments, but was similarly observed by Turns et al.[7] when recording the size change of aluminum droplet combustion using high-speed cinematography. They found that within 0.5 s of the beginning of combustion, aluminum will retain the original size, then suddenly drop to about 70% of the original size and further slowly decrease in diameter thereafter. The 2-s combustion was reported to give 98% Al_2O_3. The implication of these results will be discussed shortly.

As the aluminum agglomerate burns, it converts a large fraction Fs of its mass to smoke, and the rest to Al/Al_2O_3 agglomerates that were eventually collected in QPCB experiments. If one aluminum agglomerate is assumed to evolve into smoke plus one fully burned residual droplet of diameter D, then mass conservation shows that the ratio of D to initial agglomerate size D_{ag} is

$$\beta = D/D_{ag} = \beta_0(1 - Fs)^{1/3} \tag{3}$$

where

$$\beta_0 = (1.8895R)^{1/3}$$

$$R = \rho_{Al}/\rho_{Al_2O_3}$$

$R \cong 0.59$ if both the initial aluminum agglomerate and final residual droplet are at the flame temperature 3611 K. With the data of Fs in Table 1 obtained from unburned Al and Eq. (2), the predicted β from Eq. (3) is shown. The average β are 0.739 $\pm$ 0.021 and 0.727 $\pm$ 0.016 at 300 and 1000 psi, respectively, which are closer to the upper limit (60–80%) of the typical range, and consistent with the measurements trend of Turns et al.[7] and Salita.[8] The average Fs are 0.637 $\pm$ 0.031 and 0.655 $\pm$ 0.023 at 300 and 1000 psi, respectively, which are closer to the lower limit (60–80%) the oxide mass should be smoke for aluminized propellants. Both results are consistent with the measured large average agglomerate size for our propellants comprising a significant amount of RDX with low burning rate.

Given the data of β in Table 1, it is possible to predict the agglomerate size D by Eq. (3). Initial agglomerate size can be estimated from the Hermsen model[9]:

$$D_{ag} = \frac{35\ (\mu\text{m})}{\text{AP mass fraction} \times \text{burning rate (in./s)}} \tag{4}$$

The validity of this model may be verified by using a recent measurement data for 16% Al-69.7% AP-PBAN propellant (TP-H1148) in a small motor with 5.1 cm i.d.[10] The measured particles by the Malvern sizer at 2 cm above the propellant surface at 3.6 MPa were found to be normally distributed with a mean diameter of 132 μm. With the reported burning rate at 5.18 MPa (10 mm/s) and a pressure exponent of 0.35 (see Table 1 of Ref. 10), the burning rate at 3.6 MPa was calculated as 8.8 mm/s. Substituting the available data in Eq. (4) gives D_{ag} = 144.9 μm, which is 9.8% greater than the measured

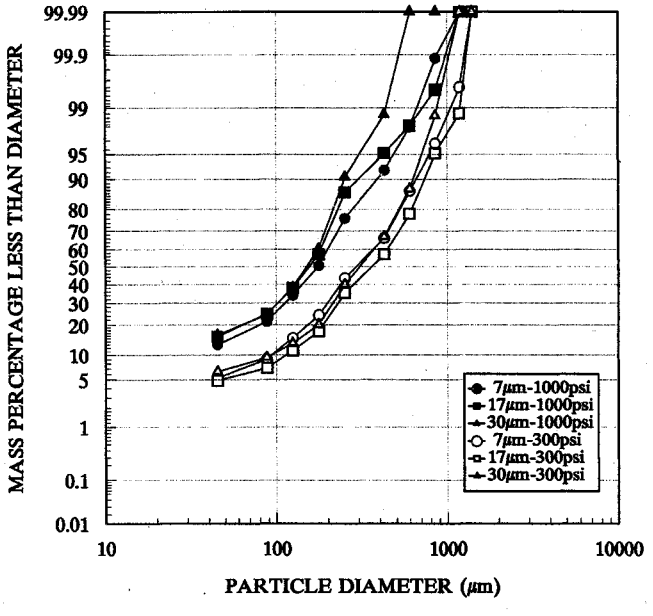

Fig. 2 Effect of Al size and pressure on agglomerate size distribution under an average quench distance of 7 mm.

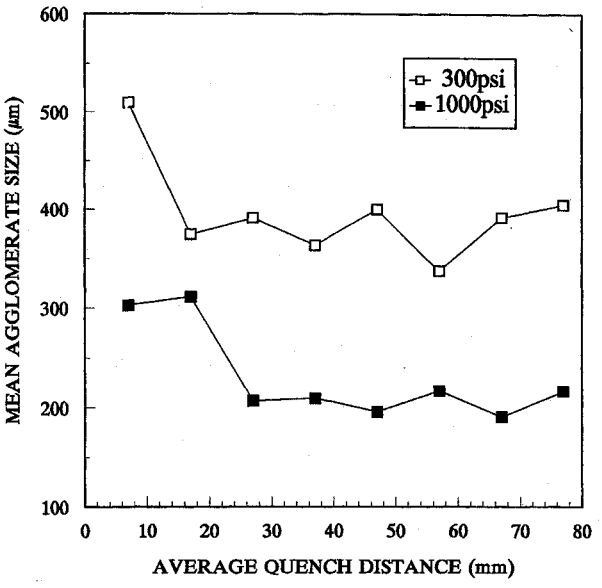

Fig. 3 Effect of pressure on mean agglomerate size of 7-μm Al propellant under different quench distances.

Table 1 Measured mean agglomerate size, smoke fraction, and predicted agglomerate diameter ratio at different quench distances and pressures

Pressure, psi	Average quench distance, mm																
	7	7	17	17	27	27	37	37	47	47	57	57	67	67	77	77	Mean ± σ_{n-1}
300																	
D_{exp}, μm	510	510	375	374	398	383	358	368	427	372	351	323	366	417	356	453	——
Fs	——	——	0.639	0.579	0.676	0.626	0.645	0.634	0.587	0.670	0.612	0.688	0.651	0.632	0.646	0.637	0.637 ± 0.031
β	——	——	0.739	0.777	0.712	0.747	0.734	0.742	0.772	0.717	0.756	0.704	0.730	0.743	0.734	0.740	0.739 ± 0.021
1000																	
D_{exp}, μm	307	299	294	329	202	211	222	197	199	193	226	207	195	187	207	226	——
Fs	——	——	——	——	0.638	0.645	0.684	0.643	0.650	0.641	0.654	0.625	0.694	0.673	0.630	0.682	0.655 ± 0.023
β	——	——	——	——	0.739	0.734	0.707	0.736	0.731	0.737	0.728	0.748	0.699	0.715	0.745	0.708	0.727 ± 0.016

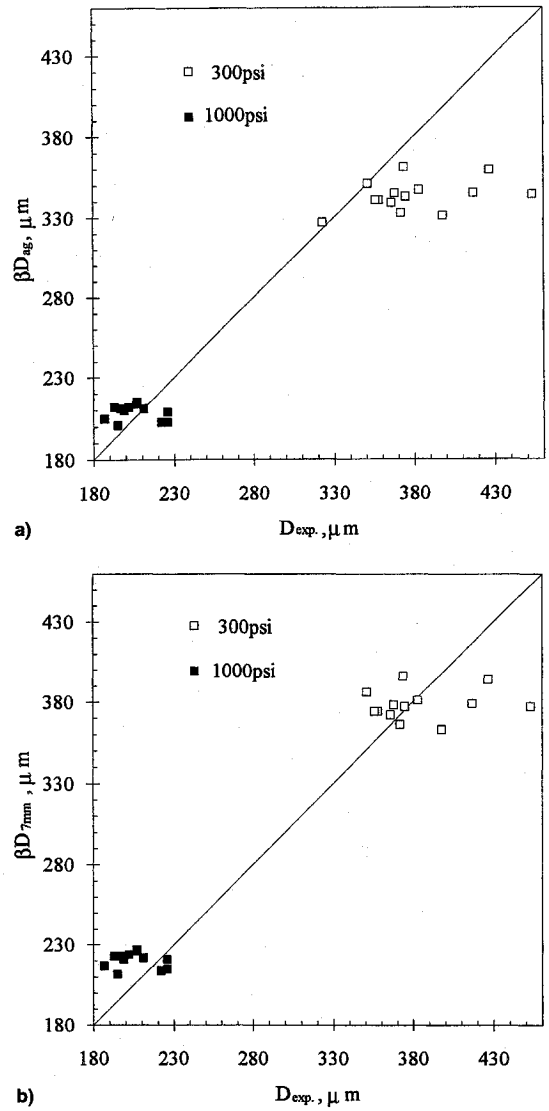

Fig. 4 a) Comparison between measured agglomerate size and the ones from predicted β and D_{ag} and b) comparison between measured agglomerate size and the ones from predicted β and measured size at 7-mm-average quench distances.

value, illustrating the adequacy of Eq. (4) in that data range. The burning rates of our propellants are 0.152 and 0.246 in./s at 300 and 1000 psi, respectively. Thus, the predicted D_{ag} from Eq. (4) are 464 and 287 μm at 300 and 1000 psi, respectively. These data are reasonably close to the mean agglomerate size measured at 7-mm quench distance: 510 and 303 μm at 300 and 1000 psi, respectively, shown in Fig. 3.

Figure 4a shows the comparison between the measured agglomerate size and the predicted size using predicted β [from Eq. (3), shown in Table 1], and the predicted D_{ag} [from Eq. (4)]. Better agreements are obtained for high-pressure data than low-pressure ones. The larger measured agglomerate sizes than predicted ones at low pressure are probably attributed to the limited data available in the low-burning-rate and low-AP-fraction region, where our propellants belong, for Hermsen's model. This could reduce the prediction accuracy in that region. Figure 4b shows the comparison results when D_{ag} calculated from Eq. (4) is replaced by an agglomerate size measured at 7 mm quench distance. Better overall agreement than Fig. 4a is observed for both pressures.

Conclusions

1) Aluminized propellants with a significant portion of RDX and low burning rate will generate a larger agglomerate size compared with the abundant data for aluminized AP–rubber propellants. The agglomerate size is log-normal distributed.

2) The agglomerate sizes in QPCB experiments remain constant within the 7–17 mm average quench distance, then decrease suddenly to a near constant size for greater quench distances. The average diameter ratios β are 0.739 ± 0.021 and 0.727 ± 0.016 at 300 and 1000 psi, respectively, which are close to the upper limit of the conventionally recognized range of 60–80%. The average fraction of smoke-generated *Fs* are 0.637 ± 0.031 and 0.655 ± 0.023 at 300 and 1000 psi, respectively, which are close to the low limit of the conventionally recognized range of 60–80%. Both β and *Fs* of aluminized AP/RDX/HTPB propellants are consistent with the result given in 1.

3) Hermsen's model for predicting the initial agglomerate size of propellants in low-AP-content and low-burning-rate region appears doubtful. Instead, agglomerate sizes measured at the shortest possible quench distance give better prediction of the subsequent size with the available β determined from Eq. (3).

Acknowledgments

The comments and suggestions given by one of the reviewers that led to the generation of Fig. 4a are appreciated.

References

[1]Sambamurthi, J. K., Price, E. W., and Sigman, R. K., "Aluminum Agglomeration in Solid-Propellant Combustion," *AIAA Journal*, Vol. 22, No. 8, 1984, pp. 1132–1138.

[2]Mitani, T., and Izumikawa, M., "Combustion Efficiencies of Aluminum and Boron in Solid Propellants," *Journal of Spacecraft and Rockets*, Vol. 28, No. 1, 1991, pp. 79–84.

[3]Churchill, H. I., Fleming, R. W., and Cohen, N. S., "Aluminum Behavior in Solid Propellant Combustion," Lockheed Propulsion Co., AFRPL-TR-74-13, Redlands, CA, March 1974.

[4]Braithwaite, P. C., Christensen, W. N., and Daugherty, V., "Quench Bomb Investigation of Aluminum Oxide Formation from Solid Rocket Propellants (pt. I): Experimental Methodology," *25th JANNAF Combustion Meeting* (Huntsville, AL), Chemical Propulsion Information Agency, Johns Hopkins Univ., Applied Physics Lab., CPIA-Pub-498-V1, Laurel, MD, 1988, pp. 175–184.

[5]Salita, M., "Quench Bomb Investigation of Aluminum Oxide Formation from Solid Rocket Propellants (pt. II): Analysis of Data," *25th JANNAF Combustion Meeting* (Huntsville, AL), Chemical Propulsion Information Agency, Johns Hopkins Univ., Applied Physics Lab.,

CPIA-Pub-498-V1, 1988, pp. 185–197.
[6]Liu, T. K., Perng, H. C., Luh, S. P., and Liu, F., "Aluminum Agglomeration in AP/RDX/Al/HTPB Propellant Combustion," *Journal of Propulsion and Power*, Vol. 8, No. 6, 1992, pp. 1177–1184.
[7]Turns, S. R., Wong, S. C., and Ryba, E., "Combustion of Aluminum-Based Slurry Agglomerates," *Combustion Science and Technology*, Vol. 54, Nos. 1–6, 1987, pp. 299–318.
[8]Salita, M., "Survey of Recent Al_2O_3 Droplet Size Data in Solid Rocket Chambers, Nozzles, and Plumes," 31st JANNAF Combustion Meeting (Sunnyvale, CA), Oct. 1994.
[9]Hermsen, R. W., "Aluminum Combustion Efficiency in Solid Rocket Motors," AIAA Paper 81-0038, Jan. 1981.
[10]Laredo, D., McCrorie, J. D., II, Vaughn, J. K., and Netzer, D. W., "Motor and Plume Particle Size Measurements in Solid Propellant Micromotors," *Journal of Propulsion and Power*, Vol. 10, No. 3, 1994, pp. 410–418.

Shock-Tunnel Investigation of Hypervelocity Free Shear Layers in a Planar Duct

D. R. Buttsworth* and R. G. Morgan†
University of Queensland, Queensland 4072, Australia

Introduction

WHILE fully developed mixing layers provide a useful configuration for fundamental investigations of turbulent compressible mixing,[1] other configurations such as transverse orifice injection,[2] wall slot injection,[3] and central strut injection,[4] are important because they directly model certain features of scramjet combustor flowfields. In the present work, hypervelocity mixing was studied using a central strut injection model of a scramjet. The term hypervelocity is used to distinguish the current study (in which the maximum flow velocity was approximately 4.3 $km \cdot s^{-1}$) from earlier work[5] in which the maximum flow velocity was much lower (approximately 1.3 $km \cdot s^{-1}$). The free shear layers were not fully developed and the majority of the pitot pressure measurements were made after the two mixing layers (from either side of the strut injector) met on the centerline of the injected stream. The present investigation examines the development of compressible mixing in the presence of relatively large hypervelocity boundary layers. This configuration differs significantly from the compressible mixing-layer configurations studied recently,[1,6] but is relevant because of the relatively high Reynolds number conditions anticipated in scramjet combustors.

Experiment

The T4 reflected shock tunnel and contoured hypersonic nozzle was operated at four different conditions with a nitrogen test gas. For the present experiments, disturbances that alter the nozzle reservoir pressure during the test time[7] were minimized through the appropriate selection of driver gas mixtures of helium and argon.[8] A planar duct that was 164 mm high and 80 mm wide was located centrally at the exit of the hypersonic nozzle (Fig. 1). A secondary stream from the base of a central strut was injected parallel to the shock tunnel (or primary) stream. The strut injector was 152 mm long and 7.59 mm high with an asymmetric 6.6-deg wedge at the leading edge. Inviscid calculations indicated that the asymmetric strut injector geometry should have a negligible effect on the flow conditions on either side of the strut injector.[8] The strut injector had a small contoured nozzle, which was designed (using the method of characteristics) to produce a uniform Mach 3 flow. The throat of the injection nozzle was 1.74 mm high, and the trailing edges were 0.19 mm thick. Hydrogen was supplied to the injector by a Ludwieg tube. Estimates of the primary and secondary stream conditions are given in Table 1 (additional details may be found in Ref. 8).

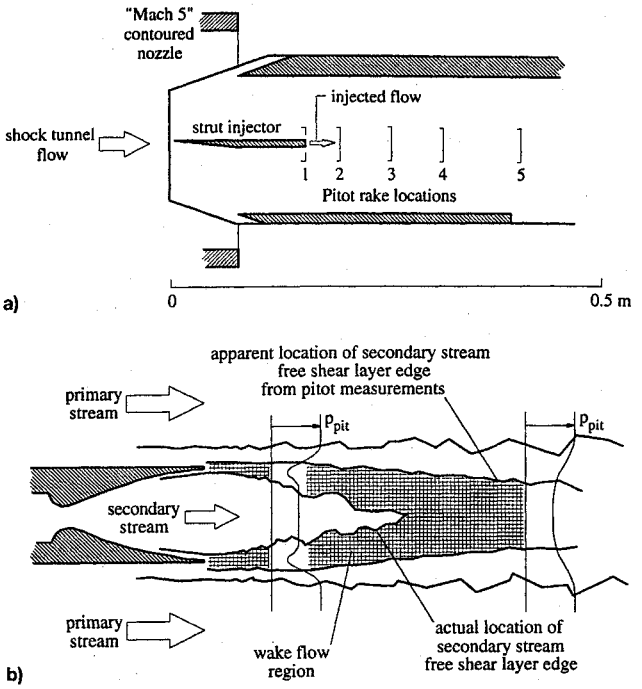

Fig. 1 Illustrations showing details of the planar duct model and the free shear-layer configuration. Stations 1–5 correspond to pitot rake measurements at x = 0, 40, 100, 160, and 250 mm: a) side view of the planar duct and b) schematic illustration of free shear-layer formation.

Pitot pressure measurements were obtained using piezoelectric transducers in a pitot rake with seven probes.[8] Each probe had an external diameter of 2.65 mm, an internal diameter of 2.04 mm, and an overall cavity length of approximately 27.5 mm. To determine the pressure indicative of the flow at the pitot rake location during the test time, a degree of averaging was necessary, because there was some acoustic resonance in the cavity ahead of the transducer. During the analysis of the pitot pressure signals, due caution was exercised to ensure that the results were influenced by neither the starting processes prior to the commencement of the useful test time, nor the slight decay in stagnation pressure, nor driver gas contamination that terminated the usable test flow.[8]

Results

Distributions of pitot pressure at five stations (see Fig. 1), corresponding to distances downstream from the injector trailing edge of 0, 40, 100, 160, and 250 mm, are presented in Fig. 2 for each of the operating conditions. At each station and condition, results are given for at least two shock-tunnel runs. (The pitot rake was offset vertically to improve the resolution of the measurements.)

The primary stream pitot pressure measured at station 2 was generally higher than at the other stations. Gun-tunnel experiments performed at similar Mach and Reynolds numbers with the same model demonstrated similar effects.[5] The increase in primary stream pitot pressure is attributed to the leading-edge shock waves from the duct side walls (because of boundary-

Received Oct. 27, 1995; revision received April 26, 1996; accepted for publication April 30, 1996.

*Postgraduate Student, Department of Mechanical Engineering; currently at the University of Oxford, Department of Engineering Science, Oxford, England, UK.
†Associate Professor, Department of Mechanical Engineering.